

Quasi-Particle Spectrum around a Single Vortex in Superconductors

— *s*-Wave Case —

Masaru KATO^{*)} and Kazumi MAKI^{*,**)}

*Department of Mathematical Sciences, Osaka Prefecture University
Sakai Osaka 599-8531, Japan*

**Department of Physics and Astronomy, University of Southern California
Los Angeles, CA 90089-0484, USA*

(Received December 20, 1999)

Making use of the Bogoliubov-de Gennes equation, we study the quasi-particle spectrum and the vortex core structure of a single vortex in quasi 2D *s*-wave superconductors for small $p_F \xi_0$, where p_F is the Fermi momentum and $\xi_0 = v_F/\Delta_0$ is the coherence length ($\hbar = 1$). During our numerical calculation the particle number is conserved for each $p_F \xi_0$. In particular, we find that there are only 1 or 2 bound states for $p_F \xi_0 = 1$. Also, for $p_F \xi_0 = 1$, the Kramer-Pesch effect ceases to exist at around $T/T_c \simeq 0.3$.

§1. Introduction

There are renewed interests in vortex structure since the discovery of high T_c cuprate superconductors. It is possible that the superconductivity of high T_c cuprates can be characterized as *d*-wave superconductivity^{1), 2)} and is very close to the quantum limit.^{3), 4)}

Schopohl and Maki previously studied the quasi-particle spectrum around a single vortex line in terms of a quasi-classical equation^{5), 6)} and predicted a clear four-fold symmetry for a *d*-wave superconductor.⁷⁾ Then, a beautiful STM study of vortices in YBCO monocrystals was reported.⁸⁾ There are several interesting results of these studies. First, it was found that the quasi-particle spectrum exhibits circular symmetry; there is no trace of four-fold symmetry Second, there appears to be only a single bound state with energy $\approx \frac{1}{4}\Delta(0)$, where $\Delta(0)$ ($= 260$ K) is the superconducting order parameter at $T = 0$ K. A similar bound state energy was observed earlier by a far-infrared magneto-transmission from a YBCO film by Karraï et al.⁹⁾ According to the analysis of bound states around the vortex core by Caroli and co-workers,¹⁰⁾ there should be thousands of bound states. Of course, in usual *s*-wave superconductors we have $p_F \xi_0 \approx 10^3 \sim 10^4$, where p_F is the Fermi momentum and $\xi_0 = v_F/\Delta(0)$ is the coherence length ($\hbar = 1$). Thus perhaps the single bound state in YBCO suggests $p_F \xi_0 \approx 1$.³⁾ At first sight this suggestion seems outrageous, since this implies $E_F \approx 200 \sim 500$ K in YBCO. By analyzing the spin gap at $T = 0$ K observed in YBCO monocrystals with inelastic neutron scattering

^{*)} E-mail: kato@ms.osakafu-u.ac.jp

^{**) E-mail: kmaki@usc.edu}

by Rossat-Mignod et al.,¹¹⁾ we can deduce chemical potential μ given as¹²⁾

$$\mu = -345(x - 0.45) \text{ K}, \quad (1.1)$$

where x is the oxygen dopage corresponding to $\text{YBa}_2\text{Cu}_3\text{O}_{6+x}$. Then, for optimally doped YBCO we obtain $\mu = -190 \text{ K}$.

In Döttinger et al.,⁴⁾ the flux-flow resistance of 60 K YBCO measured by Matsuda et al.¹³⁾ is analyzed, and they identified the Kramer-Pesch effect characteristic of a superconductor in the clean limit.^{14), 15)} On the other hand, apparently the Kramer-Pesch effect is absent in 90 K YBCO,¹³⁾ implying again that perhaps 90 K YBCO is in the quantum limit.⁴⁾ Here, the Kramer-Pesch effect causes the vortex core to shrink with decreasing temperature due to the decrease in the occupied bound states around the vortex line. The core size can be expressed as¹⁴⁾

$$\xi_1 = \frac{v_F}{\Delta(T)} \frac{T}{T_c}. \quad (1.2)$$

This reduction of the core size results in nonlinear conductivity.^{4), 15)} Ichioka et al.¹⁶⁾ found the Kramer-Pesch effect in *d*-wave superconductivity with the help of a semi-classical approach developed in Ref. 7).

But if $p_F \xi_0 \approx 1$, this implies that the semi-classical approach introduced in Refs. 5) and 6) is no longer reliable in studying the vortex in high T_c cuprates. For this reason, Morita, Kohmoto and Maki¹⁷⁾ studied the Bogoliubov-de Gennes equation for a single vortex in *d*-wave superconductors. Indeed, choosing $p_F \xi_0 = 1.33$, they were able to describe gross features of the STM result for YBCO. On the other hand, they have not attempted the self-consistent calculation due to numerical difficulties. Nevertheless, they discovered that there is a single bound state for $p_F \xi_0 = 1.33$ in the vortex of *d*-wave superconductors. Further, there are low energy ($E \leq 0.1\Delta$) extended states with four legs stretched in the four diagonal directions ($\pm 1, \pm 1, 0$). Recently, these extended states were rediscovered by Franz and Tešanović¹⁸⁾ in a model somewhat different from that in Ref. 17). Further, Franz and Tešanović claimed there should be no bound states, based on a different model which contains at least 3 arbitrary parameters. We believe that the absence of bound states is either due to a) neglect of particle number conservation or b) the rather strong Coulomb repulsion they introduced. It is rather surprising that Yasui and Kita¹⁹⁾ and Takigawa et al.²⁰⁾ obtained similar results as Ref. 18). Clearly in these later works, particle number conservation has been neglected. On the other hand, we have shown recently there are a few bound states within the weak coupling model, as in Ref. 17), down to $p_F \xi_0 \simeq 1$.²¹⁾ Also, this shows clearly that number conservation is crucial, as pointed out by van der Marel.²²⁾ Also, the above results confirm the validity of the work in Ref. 17) rather than that in Ref. 18).

In this paper we study the quasi-particle spectrum around a single vortex in *s*-wave superconductors in the quantum limit. This problem was previously considered by Hayashi et al.²³⁾ However, as we have mentioned, they ignored the number conservation, which is very crucial. For example van der Marel has shown that the chemical potential depends on the temperature if number conservation is imposed.²²⁾

Further, in Ref. 23), the energy cutoff is made arbitrarily, so that their result is not reliable, as we will show. Also, as we will show, the r -dependence of $\Delta(r)$ near $r = 0$ is completely determined by $u_0(r)v_0(r)$, where $u_0(r)$ and $v_0(r)$ are spinor wave functions for the lowest bound state.

In the following we concentrate on the cases $p_F\xi_0 = 1, 2$ and 4 for simplicity, and study the quasi-particle spectrum and the shape of $|\Delta(r)|$ as a function of temperature. A preliminary result on this has appeared in Ref. 24).

§2. Bogoliubov-de Gennes equation

The spatial dependence of order parameters in superconductivity is described by the Bogoliubov-de Gennes equation. We consider the case at a small magnetic field near H_{c1} , so that there is a single vortex. Therefore we can ignore the vector potential. In this case, the Bogoliubov-de Gennes equation becomes

$$\left(-\frac{1}{2m_e} \nabla^2 - \mu \right) u_n(\mathbf{r}) + \Delta(\mathbf{r}) v_n(\mathbf{r}) = E_n u_n(\mathbf{r}), \quad (2.1a)$$

$$- \left(-\frac{1}{2m_e} \nabla^2 - \mu \right) v_n(\mathbf{r}) + \Delta^*(\mathbf{r}) u_n(\mathbf{r}) = E_n v_n(\mathbf{r}), \quad (2.1b)$$

where $u_n(\mathbf{r})$ and $v_n(\mathbf{r})$ are quasi-particle wave functions.

We take the z -axis to be along the vortex line. We consider the nearly two-dimensional case for simplicity, where the kinetic term associated with the z direction is negligible. In the following, we merely consider the two-dimensional case, and we use cylindrical coordinates. Taking the gauge as $\Delta(\mathbf{r}) = |\Delta(r)|e^{-i\theta}$, the angular momentum of each eigenstate becomes half of an odd integer, $m + \frac{1}{2}$.¹⁰⁾ Then $u_n(\mathbf{r})$ and $v_n(\mathbf{r})$ become as follows;

$$u_n(r, \theta) = u_{nm}(r) \frac{e^{im\theta}}{\sqrt{2\pi}}, \quad (2.2a)$$

$$v_n(r, \theta) = v_{nm}(r) \frac{e^{i(m+1)\theta}}{\sqrt{2\pi}}. \quad (2.2b)$$

Following Gygi and Schlüter,²⁵⁾ we apply the Fourier-Bessel expansion with basis

$$\phi_{mj}(r) = \frac{\sqrt{2}}{R J_{m+1}(\alpha_{jm})} J_m(\alpha_{jm} \frac{r}{R}) \quad (2.3)$$

to $u_{nm}(r)$ and $v_{nm}(r)$, where α_{jm} is the j -th positive zero of the Bessel function of m -th order, $J_m(x)$. Then the wave functions become as

$$u_{nm}(r) = \sum_j u_{nmj} \phi_{mj}(r), \quad (2.4a)$$

$$v_{nm}(r) = \sum_j v_{nmj} \phi_{m+1j}(r). \quad (2.4b)$$

Here, the boundary condition is such that wave functions are zero at the edge of the

disk with radius R . Then the Bogoliubov-de Gennes equation becomes

$$\left[\frac{1}{2m_e} \left(\frac{\alpha_{jm}}{R} \right)^2 - \mu \right] u_{nmj} + \sum_{j_1} \Delta_{jj_1} v_{nmj_1} = E_{nm} u_{nmj}, \quad (2.5a)$$

$$- \left[\frac{1}{2m_e} \left(\frac{\alpha_{j_1 m+1}}{R} \right)^2 - \mu \right] v_{nmj} + \sum_{j_1} \Delta_{j_1 j} u_{nmj_1} = E_{nm} v_{nmj}, \quad (2.5b)$$

where $\Delta_{j_1 j_2}$ is given as

$$\Delta_{j_1 j_2} = \int_0^R \phi_{mj_1}(r) |\Delta(r)| \phi_{m+1 j_2}(r) r dr. \quad (2.6)$$

The order parameter is given as

$$|\Delta(r)| = g \sum_{|E_{nm}| \leq E_c} \sum_{m \geq 0} \sum_{j_1 j_2} u_{nmj_1} v_{nmj_2} \phi_{mj_1}(r) \phi_{m+1 j_2}(r) [1 - 2f(E_{nm})], \quad (2.7)$$

where g is the interaction constant, E_c is the cutoff energy, and $f(E)$ is the Fermi distribution function.

Also we impose particle number conservation,

$$N = 2 \int \sum_n \left\{ |u_n(\mathbf{r})|^2 f(E_n) + |v_n|^2 (1 - f(E_n)) \right\} d^2 \mathbf{r}, \quad (2.8a)$$

$$= 2 \sum_j \sum_{nm} \left[|u_{nmj}|^2 f(E_{nm}) + [|v_{nmj}|^2 (1 - f(E_n))] \right], \quad (2.8b)$$

where N is the total number of particles. The chemical potential is determined by this equation. Here N is the particle number of the normal state with specified p_F at $T = 0$. We solve these equations, Eqs. (2.5), (2.7) and (2.8), self-consistently. We fix the cutoff energy ($E_c = 5\Delta_0$ for the case of largest Fermi momentum) and the interaction constant, and choose the Fermi momentum p_F so that $p_F \xi_0 = 1, 2$ and 4.

§3. Results

In the numerical calculation, the radius of boundary is taken as $R = 10\xi_0$, and maximum angular momentum and number of zero points of the Bessel functions are taken so that all of the quasi-particle states within the cutoff energy are taken into the calculation.

Before proceeding to the numerical results, here we discuss the temperature dependence of the chemical potential for the superconducting state. The chemical potentials for the normal state (μ_n) and the superconducting state (μ_s) of the two-dimensional system are given as²²⁾

$$\beta \mu_n(T) = \ln \left(e^{\beta \mu_n(0)} - 1 \right), \quad (3.1)$$

$$2\mu_n(0) = \mu_s(T) + E_c - \sqrt{E_c^2 + \Delta(T)^2} + \sqrt{\mu_s(T)^2 + \Delta(T)^2} - \frac{2}{\beta} \ln \frac{1 + e^{-\beta \sqrt{E_c^2 + \Delta(T)^2}}}{1 + e^{-\beta \sqrt{\mu_s(T)^2 + \Delta(T)^2}}} + \frac{2}{\beta} \ln \left(1 + e^{-\beta E_c} \right). \quad (3.2)$$

The temperature dependences of the chemical potential for $p_F\xi = 1$ and 4 are shown in Fig. 1. As pointed out by van der Marel,²²⁾ the chemical potential decreases with decreasing temperature in the superconducting state. This is opposite to the behavior in the normal state. As we can see from the figure for $p_F\xi_0 = 1$, the chemical potential becomes very small in the superconducting state, and the chemical potential of the normal state drops significantly from $T = 0$ to $T = T_c$. For larger p_F , this temperature dependence of the chemical potential becomes much weaker. Therefore the temperature dependence and the p_F dependence of physical quantities may change from those with the constant chemical potential calculation in the quantum limit.

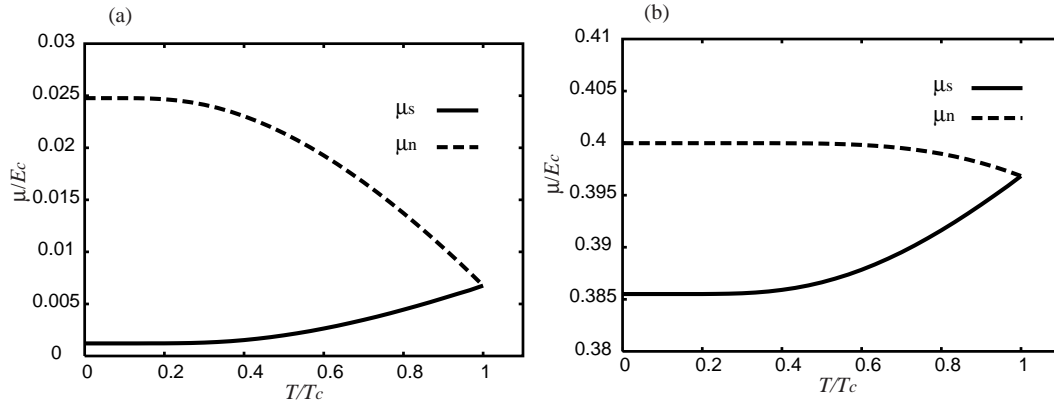


Fig. 1. Temperature dependence of the chemical potential for $p_F\xi_0 = 1$ (a) and $p_F\xi_0 = 4$ (b). The solid curve is the chemical potential for the superconducting state, and the broken curve is that for the normal state.

3.1. Temperature dependence of order parameter

The temperature dependence of the order parameter is shown in Fig. 2. Near the boundary $r/\xi_0 = 10$, the order parameter goes to zero, and there is a peak before that. These are effects from the boundary condition and the finite size. But the core structures are not affected by the boundary condition.

For $p_F\xi_0 = 4$ at low temperature ($T/T_c \leq 0.1$) there is a shoulder in $|\Delta(r)|$ at the vortex core. This feature comes from bound states in the vortex core. This can be seen from Fig. 3, where contributions of the scattering states and the bound states are shown separately.

For $p_F\xi_0 = 1$, the peak position of the contribution to the order parameter is located slightly outside of the vortex core. Therefore the core structure is not so strongly affected by the bound states. For larger $p_F\xi_0 (\sim 16)$, Hayashi et al.²³⁾ demonstrated the oscillation of the order parameter on the inside of the vortex core. They argued that this oscillation is Friedel oscillation, but from our figures it appears that the origin of the oscillation is the discreteness of the bound states.

Slightly increasing the temperature, the bound state contribution decreases rapidly, and the scattering state contribution remains almost the same. In this temperature range, the core size is dominated by the bound states. Above this

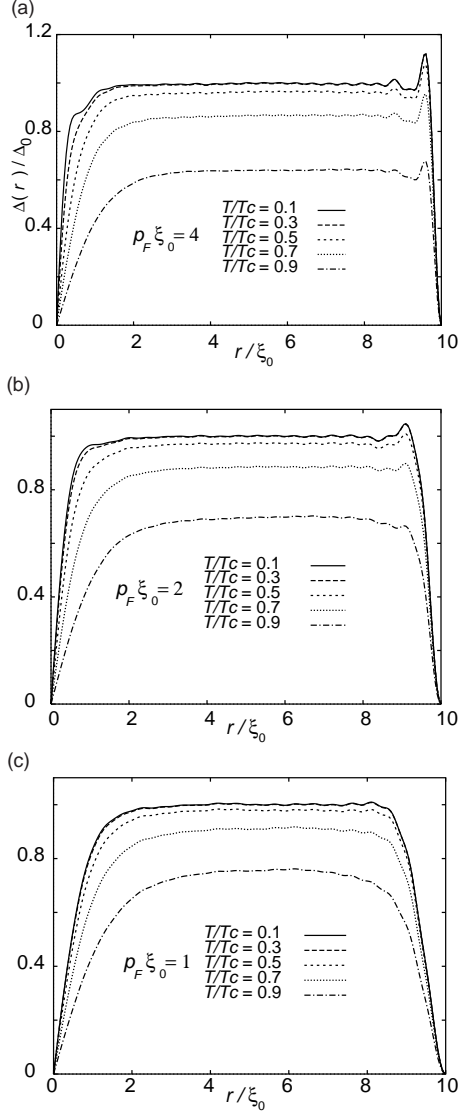


Fig. 2. The temperature dependence of the order parameter $\Delta(r)$ for (a) $p_F\xi_0 = 4$, (b) $p_F\xi_0 = 2$ and (c) $p_F\xi_0 = 1$. The order parameter is normalized with $\Delta_0 = \Delta(r = 5.5\xi_0, T = 0)$ for each $p_F\xi_0$.

temperature region, the scattering state contribution decreases with increasing temperature, which is the same behavior as that of the order parameter of the uniform solution.

We also plot the quasi-particle wave functions $u_{n\mu}(r)$ and $v_{n\mu}(r)$ of three bound states for $p_F\xi_0 = 4$ in Fig. 4. From these figures, it can be seen that main contribution to the core structure comes from the lowest energy bound state.

Also, we can see that $u(r)$ of the lowest energy bound state behaves like an

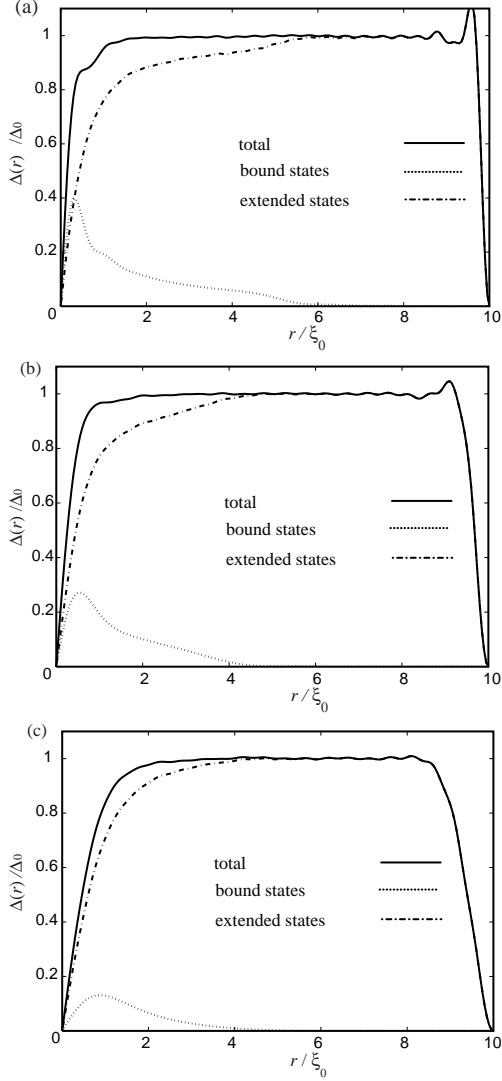


Fig. 3. Contributions from the bound states and the scattering states to the order parameter for (a) $p_F\xi_0 = 4$, (b) $p_F\xi_0 = 2$ and (c) $p_F\xi_0 = 1$, where $\Delta_0 = \Delta(r = 5.5\xi_0, T = 0)$.

s-wave function, and $v(r)$ behaves like *p*-wave function. Similar behavior also can be seen for the second and third lowest bound states. They belong to the angular

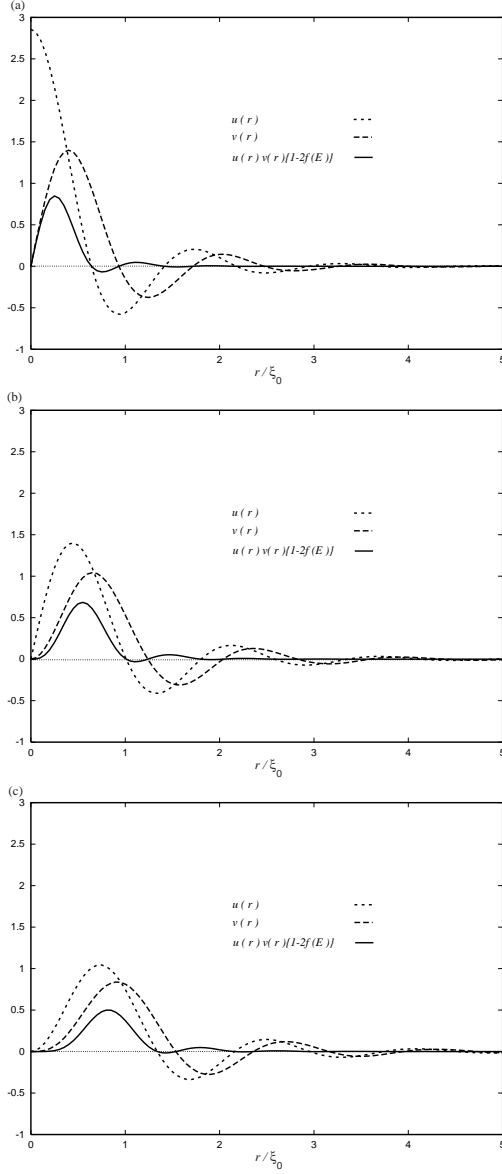


Fig. 4. The quasi-particle wave functions $u(r)$ and $v(r)$ and their product with a thermal factor for (a) the first, (b) the second and (c) the third of the lowest energy bound states.

momentum m and $m + 1$ states, respectively.

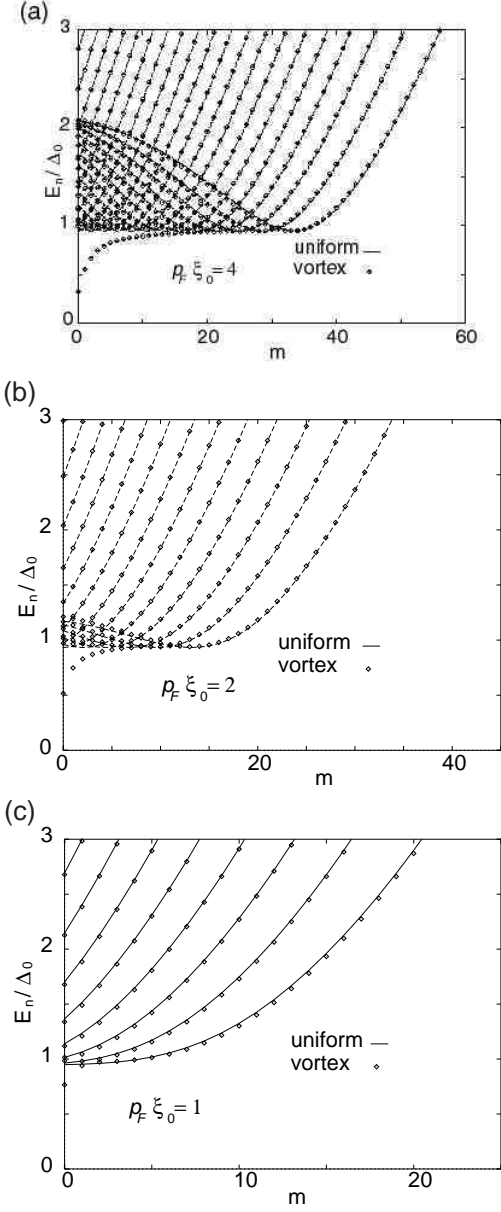


Fig. 5. The quasi-particle spectrum of the vortex state (\diamond) and the uniform state (dashed curves) for (a) $p_F\xi_0 = 4$, (b) $p_F\xi_0 = 2$ and (c) $p_F\xi_0 = 1$.

3.2. Quasi-particle spectrum

In Fig. 5 we give quasi-particle energies with angular momentum $m + \frac{1}{2}$, and we also plot those of the uniform state in order to compare the vortex state and the uniform state. For small angular momentum, the lowest energy states become bound states, lowering their energies and slightly increasing the energies of higher energy states. For larger angular momentum, the quasi-particle energy is almost same for vortex and uniform states, and there is no bound state.

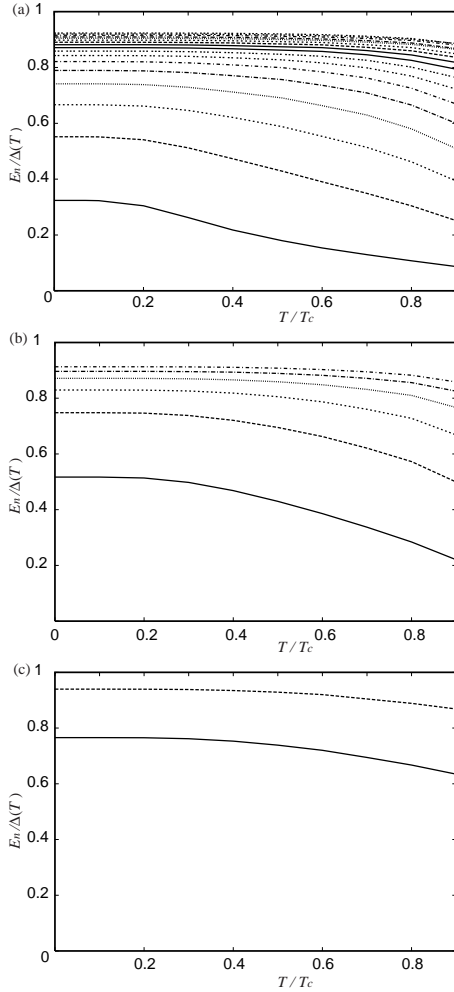


Fig. 6. The temperature dependence of the quasi-particle energies of the bound states in the vortex state. The energies are normalized by the order parameter $\Delta(T)$ at $r/\xi_0 = 5.5$. (a), (b) and (c) are for $p_F\xi_0 = 4$, $p_F\xi_0 = 2$ and $p_F\xi_0 = 1$, respectively.

their result shows that the energy increases with decreasing temperature even at

Although it is difficult to determine the boundary of these two cases in the angular momentum, the number of bound states may be counted as 18 for $p_F\xi_0 = 4$, 5 for $p_F\xi_0 = 2$, and 1 or 2 for $p_F\xi_0 = 1$. Compared with our previous calculation without number conservation, the number of the bound states decreases. This effect is clearer for smaller $p_F\xi_0$.

Such a relation between the number of the bound states and Fermi momentum is important for d -wave superconductors, because the local density of states changes greatly due to this relation. Therefore, it is worthwhile to point out this relation for the s -wave case, and in order to obtain the correct relation, our number conserved calculation is needed.

The temperature dependence of the quasi-particle energy is shown in Fig. 6. In this figure we plot the quasi-particle energies of several bound states normalized with the order parameter $\Delta(T)$ at $r = 5.5\xi_0$. From this figure we can see that for smaller $p_F\xi_0$ and higher energy states, the quasi-particle energy varies in proportion to the order parameter with temperature. But for lower energy states with larger $p_F\xi_0$, the quasi-particle energy increases rapidly with decreasing temperature and becomes constant at low temperature. This behavior of the energy of the lowest bound state was previously noted by Gygi and Schlüter²⁵⁾ for much larger $p_F\xi_0$, but

low temperature because of the large value of $p_F\xi_0$.

3.3. Core radius

As mentioned in 3.1, the core structure depends on the bound states. As defined by Kramer and Pesch,¹⁴⁾ we calculate the core radius ξ_1 as

$$\frac{1}{\xi_1} = \lim_{r \rightarrow 0} \frac{\Delta(r)}{r \Delta_0}, \quad (3.3a)$$

$$= \frac{g}{\Delta_0} \sum_{E_{n0} \leq E_c} \sum_{j_1 j_2} u_{n0j_1} v_{n0j_2} [1 - 2f(E_{n0})] \phi_{0j_1}(0) \frac{d\phi_{1j_2}}{dr}(0). \quad (3.3b)$$

We plot total ξ_1^{-1} and the contribution from the scattering states to ξ_1^{-1} in Fig. 7.

The temperature dependence of ξ_1 is almost linear in the intermediate temperature region, according to Kramer and Pesch.¹⁴⁾ For $p_F\xi_0 = 4$, there is a substantial decrease of the core radius at low temperature because of empty bound states. Although for smaller $p_F\xi_0$ there is a bound state contribution, the peak position for its contribution to the order parameter is nearly at the edge of the core. Therefore the core radius is not strongly affected. But for large $p_F\xi_0$, the peak of the contribution of the bound states is well inside the core, so the core radius shrinks significantly.

Our result exhibits saturations of ξ_1^{-1} at $T/T_c \approx 0.1$ for $p_F\xi_0 = 4$, at $T/T_c \approx 0.2$ for $p_F\xi_0 = 2$ and at $T/T_c \approx 0.3$ for $p_F\xi_0 = 1$. This saturation comes from the disappearance of the occupied bound states at low temperature. In Fig. 3 in Ref. 23), ξ_1 is found to saturate at $T/T_c \approx 0.1$ for small $p_F\xi_0$. However, the authors of that work did not impose the particle number conservation condition, and therefore the temperature dependence of ξ_1 is different from that in our result.

3.4. Current density and magnetic field

The current density is calculated from

$$\mathbf{j}(\mathbf{r}) = \frac{e}{2m_e i} \sum_{nm} \{ f(E_{nm}) u_{nm}^*(\mathbf{r}) \nabla u_{nm}(\mathbf{r}) + [1 - f(E_{nm})] v_{nm}(\mathbf{r}) \nabla v_{nm}^*(\mathbf{r}) - \text{h.c.} \}. \quad (3.4)$$

There exists rotational symmetry, so the current has only a θ component:

$$j_\theta(r) = \frac{e}{m_e} \sum_{nm} \left\{ f(E_{nm}) \frac{m}{r} |u_{nm}(r)|^2 - [1 - f(E_{nm})] \frac{m+1}{r} |v_{nm}(r)|^2 \right\}. \quad (3.5)$$

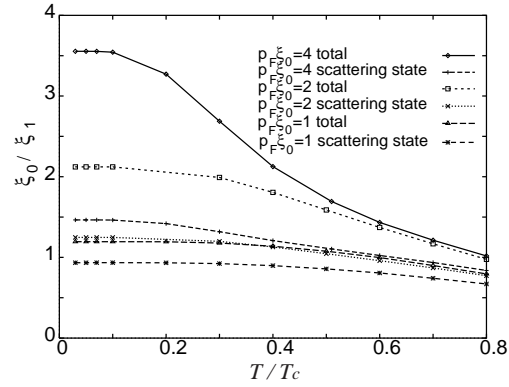


Fig. 7. The temperature dependence of ξ_1^{-1} for $p_F\xi_0 = 1, 2$ and 4 . Also contributions from scattering states for each $p_F\xi_0$ are plotted.

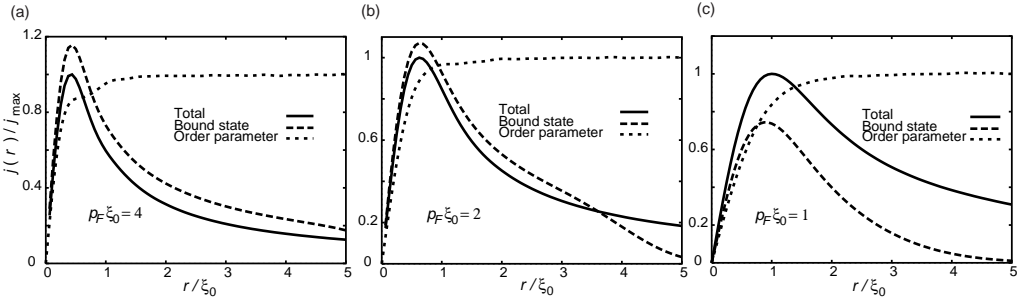


Fig. 8. The current density at $T = 0.1T_c$ for (a) $p_F\xi_0 = 4$, (b) $p_F\xi_0 = 2$ and (c) $p_F\xi_0 = 1$. The current density is normalized by its maximum value. The order parameter is also shown for comparison.

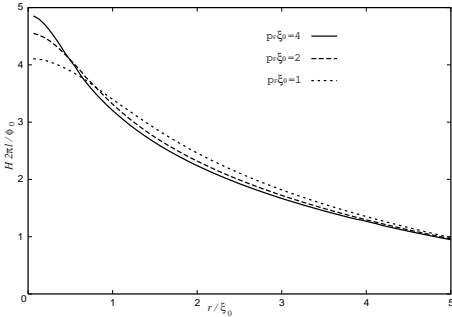


Fig. 9. The spatial dependence of the magnetic field H at $T = 0.1T_c$ for $p_F\xi_0 = 1, 2$ and 4 .

We show this current density at $T = 0.1T_c$ in Fig. 8 for each $p_F\xi_0$. We see that the peak position of the current density is almost the same as the peak position of the lowest energy bound state. Therefore, for a smaller value of $p_F\xi_0$, the peak is located farther from the vortex core. Also, for smaller $p_F\xi_0$, the contribution of the scattering states is the same as that of the bound states, although for larger $p_F\xi_0$ the contribution of the scattering states is op-

posite to that of the bound states. Therefore there is no simple relation between the core size and the peak position of the current; that is, they are not exactly the same.

From Maxwell's equations, we calculate the magnetic field parallel to the z -axis as

$$H_z(r) = \frac{4\pi}{c} \int_r^R j_\theta(r) dr. \quad (3.6)$$

We have normalized this with $\phi_0/2\pi\lambda^2$, and show in Fig. 9, where $\lambda = (m_e c^2 / 4\pi n e^2)^{1/2}$ is the penetration depth and $\phi_0 = hc/2e$ is the flux quantum. From this figure, we find that for smaller $p_F\xi_0$, the distribution of the magnetic field is extended farther to the outside of the vortex core.

3.5. Local density of states

In order to compare with STM experiments, we calculate the local density of states with thermal average,

$$N(r, E) = - \sum_{nm} \{ |u_{nm}(r)|^2 f'(E_{nm} - E) + |v_{nm}(r)|^2 f'(E_{nm} + E) \}. \quad (3.7)$$

We also take the spatial average with a Gaussian distribution with standard deviation $0.1\xi_0$. This is shown in Fig. 10. In this figure there is oscillatory behavior for

$E/\Delta_0 > 1.0$, where the value of the order parameter outside the vortex core. This feature results from the finite size of our system, and it is an artifact. In addition to this, there are several peaks due to the discrete bound states for energies less than the energy gap ($E < \Delta_0$), and there is a particle-hole asymmetry, in contrast to the result of Gygi and Schlüter.²⁵⁾ Wang and MacDonald²⁶⁾ demonstrated this asymmetry by solving the lattice model, and Morita et al.¹⁷⁾ and Hayasi et al.²³⁾ pointed it out previously. At $p_F\xi_0 = 1$ there is only a peak near the energy gap, in contrast to the *d*-wave case, where for smaller $p_F\xi_0$ there are only shoulders inside of the energy gap.²¹⁾

§4. Conclusion

In summary, we have solved the Bogoliubov-de Gennes equation with the number conservation condition for a single vortex state in *s*-wave superconductors for small $p_F\xi_0$, and we have obtained the electronic structure around the vortex core. The number conservation condition strongly affects the quasi-particle spectrum and the core structure, because the chemical potential varies strongly with the temperature in the quantum limit ($p_F\xi_0 = O(1)$), especially for smaller $p_F\xi_0$. Also, we have elucidated the effect of the discrete bound states on the order parameter structure, the local density of states, the current density and the magnetic field. For smaller $p_F\xi_0$, the contribution of the bound states to $\Delta(r)$ decreases, and the actual shape of $\Delta(r)$ depends on the peak positions of the product of the wave functions of bound states. Also, the discreteness of the bound states is more apparent for smaller $p_F\xi_0$.

Recently, Sonier et al.²⁷⁾ claimed that they obtained the core size of the vortex in NbSe₂ by measuring the peak position of the current density. However, there are a few problems in their procedure. First, as we have shown, there is apparently no

Δ_0 is the average

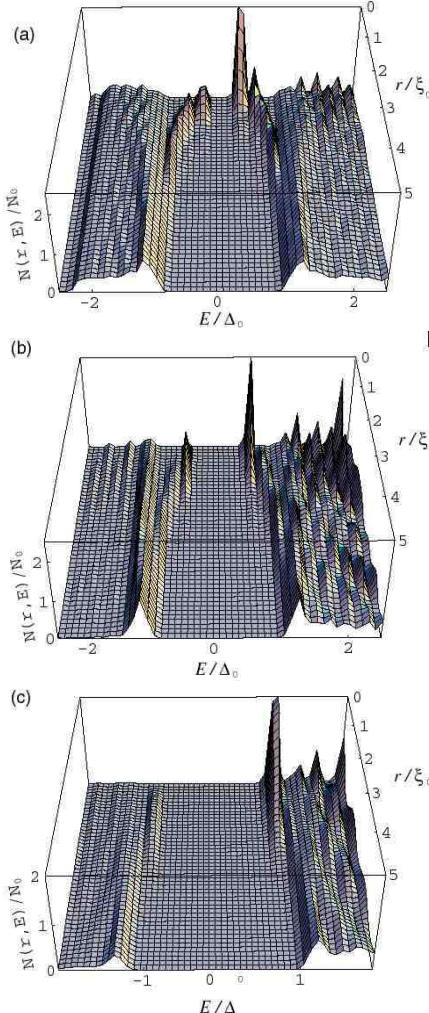


Fig. 10. The local density of states $N(r, E)$ at $T/T_c = 0.1$ for (a) $p_F\xi_0 = 4$, (b) $p_F\xi_0 = 2$ and (c) $p_F\xi_0 = 1$. $N(r, E)$ is normalized by the density of states of the normal state N_0 .

simple relation between the peak in the current density and the core size. Second, even if such a relation did exist the relation between these quantities in the clean limit would be different from that in the dirty limit, as given by the result in Ref. 27). In particular, the core size in the clean limit is much smaller than that in the dirty limit with respect to the peak position in the current density. At least those authors should have analyzed their data in light of the clean limit calculation by Gygi and Schlüter.²⁵⁾ Third, the muon spin rotation experiment measures the average of the spatial distribution of the magnetic field. Therefore it is not suited to extract the current distribution. Rather, it should be used to extract the magnetic-field dependent magnetic penetration depth, which will provide more insight into the vortex state.

As compared with the result for *d*-wave superconductors,²¹⁾ our result exhibits systematic decrease in the number of bound states with decreasing Fermi momentum. In the *d*-wave case, there are bound states and extended states around a vortex. Therefore detailed study is needed for *d*-wave superconductors. Such a calculation is now in progress.

Acknowledgements

The present work is supported by an NSF under grant number DMR 9531720. One of us (MK) is supported by the Ministry of Education, Science and Culture of Japan through the program of exchange researchers. He is grateful for the hospitality of the Department of Physics and Astronomy of the University of Southern California. Also MK appreciates useful discussions with A. Goto and A. Nakanishi.

References

- [1] C. C. Tsuei and J. R. Kirtley, *Physica* **C282-287** (1997), 4.
- [2] D. J. Van Harlingen, *Physica* **C282-287** (1997), 128.
- [3] K. Maki and H. Won, *J. Phys. I (Paris)* **6** (1996), 2317.
- [4] S. G. Döttinger, R. P. Huebener and S. Kittelberg, *Phys. Rev.* **B55** (1997), 6044.
- [5] G. Eilenbeger, *Z. Phys.* **214** (1968), 195.
- [6] A. I. Larkin and Yu. N. Ovchinnikov, *Zh. Eksp. Teor. Fiz.* **55** (1968), 2262 [*Sov. Phys. JETP* **288** (1969), 1200].
- [7] N. Schopohl and K. Maki, *Phys. Rev.* **B52** (1995), 490.
- [8] I. Maggio-Aprile, Ch. Renner, A. Erb, E. Walker and Ø. Fischer, *Phys. Rev. Lett.* **75** (1995), 2754.
- [9] K. Karraï et al., *Phys. Rev. Lett.* **69** (1992), 152; *Physica* **B197** (1994), 624.
- [10] C. Caroli, P. G. de Gennes and J. Matricon, *Phys. Lett.* **6** (1964), 307.
C. Caroli and J. Matricon, *Phys. kondens. Materie* **3** (1965), 380.
- [11] J. Rossat-Mignot et al., *Physica* **C185-186** (1991), 86; *Physica* **B186-188** (1993), 1.
- [12] H. Won and K. Maki, *Physica* **B206-207** (1995), 664.
- [13] Y. Matsuda, N. P. Ong, Y. F. Yan, J. M. Harris and J. B. Peterson, *Phys. Rev.* **B49** (1994), 4380.
- [14] L. Kramer and W. Pesch, *Z. Phys.* **269** (1974), 59.
- [15] A. I. Larkin and Yu. N. Ovchinnikov, *Sov. Phys.-JETP* **46** (1997), 155.
- [16] M. Ichioka, N. Hayashi, N. Enomoto and K. Machida, *Phys. Rev.* **B53** (1996), 15316.
- [17] Y. Morita, M. Kohmoto and K. Maki, *Phys. Rev. Lett.* **78** (1997), 4841; **79** (1997), 4514; *Europhys. Lett.* **40** (1997), 207.
- [18] M. Franz and Z. Tešanović, *Phys. Rev. Lett.* **80** (1998), 4763.
- [19] K. Yasui and T. Kita, *Phys. Rev. Lett.* **83** (1999), 4168.
- [20] M. Takigawa, M. Ichioka and K. Machida, *Phys. Rev. Lett.* **83** (1999), 3057.

- [21] M. Kato and K. Maki, *Proceedings of 22nd Int. Conf. on Low Temp. Phys.*, to appear in *Physica B; Proceedings of The LI-st Yamada Conference on Strongly Correlated Electron Systems*, to appear in *Physica B*.
- [22] D. van der Marel, *Physica* **C165** (1990), 35.
- [23] N. Hayashi, T. Isoshima, M. Ichioka and K. Machida, *Phys. Rev. Lett.* **80** (1998), 2921.
- [24] M. Kato and K. Maki, *High temperature superconductivity*, ed. S. E. Barnes et al. (American Institute of Physics, 1999), p.53.
- [25] F. Gygi and M. Schliuter, *Phys. Rev.* **B41** (1990), 822; **B43** (1991), 7609.
- [26] Y. Wang and A. H. MacDonald, *Phys. Rev.* **B52** (1995), R3876.
- [27] J. E. Sonier, R. E. Kiefl, J. H. Brewer, J. Chakhalian, S. R. Dunsiger, W. A. MacFarlane, R. I. Miller, A. Wong, G. M. Luke and J. W. Brill, *Phys. Rev. Lett.* **79** (1997), 1742.